97. Conformational Analysis of the *cis*- and *trans*-Isomers of FK506 by NMR and Molecular Dynamics

by **Dale F. Mierke, Peter Schmieder, Peter Karuso**[1]), and **Horst Kessler***

Institut für Organische Chemie, Technische Universität München, Lichtenbergstr. 4, D-8046 Garching

(21.V.91)

The potent immunosuppressant drug FK506 (**2**) has been examined by ^{1}H- and ^{13}C-NMR spectroscopy and NOE-restrained molecular dynamics to elucidate the conformation in solution. A combination of two- and three-dimensional NMR techniques was used to completely assign the ^{1}H- and ^{13}C-NMR chemical shifts of the two configurational isomers resulting from the *cis-trans* isomerization about the single amide bond. Hetero- and homonuclear coupling constants were measured to assign the diastereotopic methylene protons at C(16), C(18), and C(23). Intramolecular H–H distances were defined from NOESY spectra recorded at –30° in $CDCl_3$ and used as constraints in molecular-dynamics simulations. The conformational preferences of **2** in solution are discussed in light of the constitutional features recently proposed to be necessary for binding and activity.

Introduction. – A large effort is underway in the field of immunology to develop a better understanding of the regulation of T-lymphocyte activity. The discovery of immunosuppressants, molecules that inhibit the activation of T-cells, has produced much insight into this process. One such immunosuppressant that has been widely studied is cyclosporin A (CsA; (**1**)), a natural product isolated from fungal sources which has been

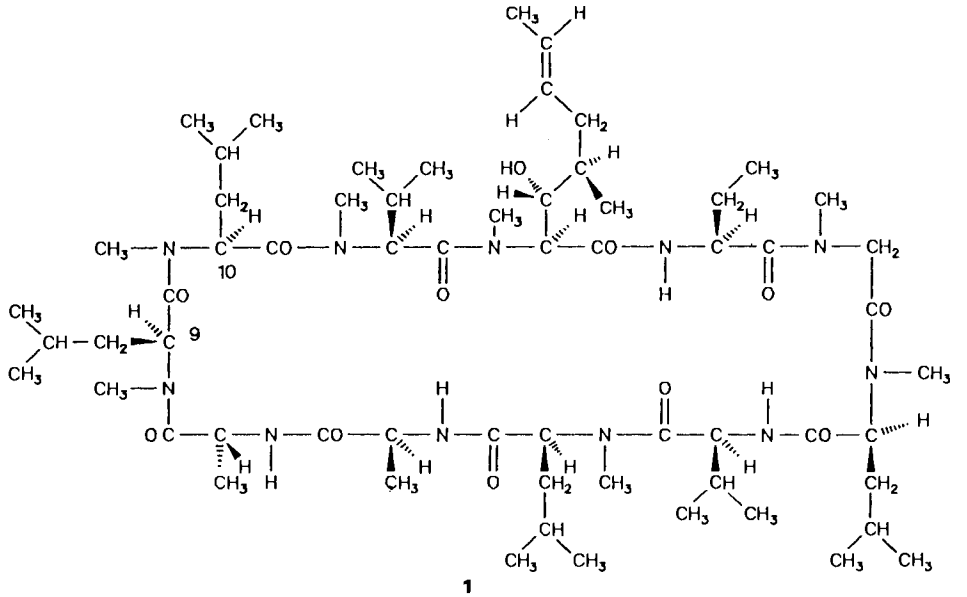

1

[1]) Present address: School of Chemistry, Macquarie University, Sydney 2109, Australia.

utilized in transplantation surgery, preventing the rejection of transplanted bone marrow and organs [1–4].

Recently, a novel 23-membered macrolide lactone, FK506 (**2**), isolated from *Streptomyces tsukubaensis* and structurally unrelated to CsA but inhibiting the activation of T-cells through a similar mechanism, was discovered [5–7]. FK506 is up to 100 times more active than CsA and is currently undergoing clinical testing.

Both **1** and **2** inhibit the activity of nuclear transcription factors, responsible for the transcription of T-cell activation genes [8] [9]. In contrast, another immunosuppressant, rapamycin (**3**) [10] which is structurally related to FK506 inhibits T-cell activation by a different mechanism, blocking T-cell proliferation primarily by suppressing lymphokine production. The X-ray structure [11] and preliminary NMR analysis [12] of rapamycin have appeared.

The receptors of these immunosuppressants have been isolated and cloned [13–15]. They form a class of proteins called immunophilins. The immunophilins which bind CsA (cyclophilin) [16] [17] and FK506 (FK binding protein, FKBP) [18–20] have been shown

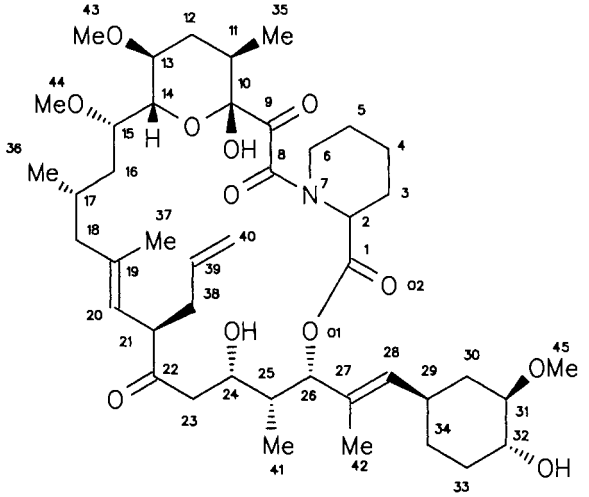

2

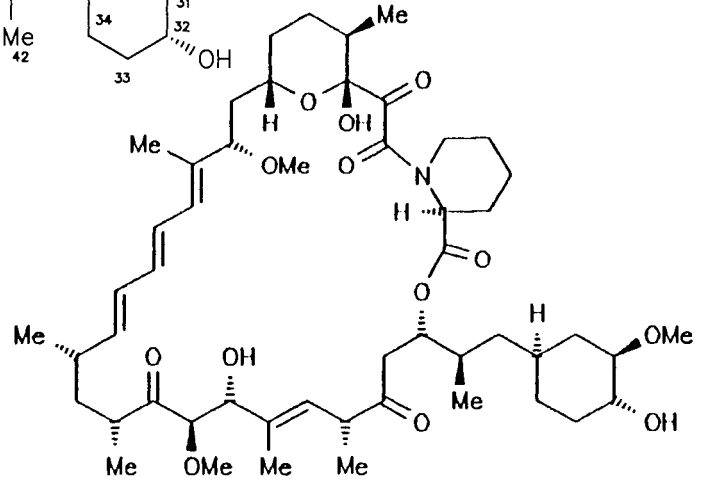

3

to be active as *cis-trans* isomerases (rotamase) [21–23]. CsA binds selectively to cyclophilin, while FK506 and rapamycin bind specifically to FKBP. There is no cross binding of the immunosuppressants (*i.e.* FK506 and rapamycin do not bind to cyclophilin and CsA does not bind to FKBP).

Binding of the substrates inhibits the rotamase activity of the immunophilins, which has led to the hypothesis that the rotamase activity is related to the inhibition of T-cell proliferation [23–25]. However, it has been pointed out that conservative estimates of the concentrations of FKBP (> 5 nM) are greater than the concentration of FK506 required for the suppression of T-cell activation (0.2 nM) [26]. This implies that there is a significant proportion of free FKBP, active as a rotamase, while T-cell activation has been inhibited. Therefore, the rotamase activity is not related to the inhibition of T-cell proliferation.

FK506 (**2**) and rapamycin (**3**) exhibit similar binding and inhibition of the rotamase activity of FKBP [27]. This has led to the suggestion that the region of constitutional similarity binds to the immunophilins ('binding region'), while the remainder of the molecule is responsible for the different mechanisms of immunosuppressant activity ('effector region') [25]. This highly plausible theory was examined with the synthesis of 506BD, an analog containing only the binding region. The selective binding of 506BD to FKBP and the lack of biological activity support the proposed domains of FK506 (**2**) and rapamycin (**3**) [25].

However, one problem with this hypothesis is the orientation about the amide bond within this binding region. In the solid state, only one rotamer is observed for each molecule: the *cis*-conformer of FK506 (**2**) [5] and the *trans*-conformer of rapamycin (**3**) [11]. In solution ($CDCl_3$) **2** exhibits both *cis*- and *trans*-isomers with populations in a ratio of 2:1 [28], while **3** is in a 4:1 ratio, with the *trans*-isomer favored [12]. In DMSO, only the *trans*-isomer of **3** is observed [29] (**2** is not soluble in DMSO). Both drugs have similar local conformations at the dicarbonyl region, but the *cis-trans* isomerization at the adjacent pipecolinic moiety produces differences in the relative orientation and accessibility of this group. This is particularly evident in the X-ray structures of the two drugs.

With this in mind, we have initiated the conformational examination of FK506 (**2**) and rapamycin (**3**) in solution, using the latest techniques in NMR and computer simulations. Recently, preliminary results from our study of **2** in $CDCl_3$ were reported [28]. Here, we report all experimental details and results, along with a reexamination of the conformation of **2** with particular attention given to the effector region. Within this region, the diastereotopic methylene protons at C(16), C(18), and C(23) have now been assigned. These assignments allow for the use of the stereospecific distance restraints derived from the NOE's. The previous study employed only the average distance restraint (averaged over both methylene protons) applied to the average position of these protons. In addition, extensive analysis of homo- and heteronuclear coupling constants has been carried out. From this analysis, the conformation of FK506 (**2**) is refined from the previous study. A similar conformational analysis of rapamycin (**3**) will be reported elsewhere [29].

Experimental. – *Nuclear Magnetic Resonance.* All NMR spectra were recorded at 243 or 300 K on *Bruker AMX-500* and *-600* spectrometers equipped with *X32* computers. The 3D spectra were calculated on a *Silicon Graphics 4D/240 SX* using the FELIX software package from Dr. *D. Hare*. A sample of FK506 (**2**; 20 mg) was dissolved in 0.5 ml of $CDCl_3$ (*Aldrich*) to give a final concentration of 33 and 17 mM for the major and minor conformational isomers, resp.

One-dimensional ^{1}H-NMR spectra were recorded with 16000 data points over a sweep width of 3300–4000 Hz and multiplied with a *Lorentzian* to *Gaussian* function prior to transformation. For the determination of temperature gradients, 6 spectra from 243 to 303 K were recorded. One-dimensional ^{13}C-NMR spectra were recorded with 64000 data points with a sweep width of 203 ppm. A *Lorentzian* line broadening of 5 Hz was applied to the FID prior to transformation.

The TOCSY spectra [30] were recorded at 300 K with a relaxation delay of 1.3 s, 16 scans, and an MLEV17 [31] mixing sequence with 2.5 ms trim pulses and a 9.5 KHz spin-locking field. Experiments with mixing times of 16, 40, and 80 ms were recorded each with 512 experiments of 2048 data points.

The ROESY spectra [32] were recorded at 300 K with a relaxation delay of 1.5 s, 32 scans, and mixing times of 60, 120, and 200 ms with 512 experiments of 2048 data points. The spin lock was achieved with a train of 2 μs pulses (15° flip angle) and 18.6 μs delay, repeated to obtain the desired mixing time [32c].

The NOESY spectrum [33] was recorded at 243 K with a relaxation delay of 1.8 s, and 80 scans. The mixing time of 90 ms was varied randomly by 15% to suppress zero quantum coherences. A sweep width of 4500 Hz was employed in both dimensions, and 512 experiments of 2048 data points were collected. The f_1 dimension was zero-filled once. After *Fourier* transform, a third-order baseplane correction was usually performed. The integral intensities of cross-peaks were measured by the integration routine within the UXNMR program.

The E. COSY spectrum [34] for three spins was recorded at 300 K with a relaxation delay of 1.3 s and a delay of 2 μs before the observation pulse. A sweep width of 3400 Hz was used in both dimensions. One thousand experiments of 4096 data points were recorded. In the f_2 dimension, shifted sinebell squared apodization was employed. The f_1 dimension was zero-filled to 2048, and a *Lorentzian* to *Gaussian* multiplication was used. The resulting spectrum was phased in f_1 and f_2 to pure antiphase absorption. The coupling constants were read directly from the expanded contour plots of relevant cross peaks.

The ^{1}H-detected ^{1}H, ^{13}C-HMQC spectrum [35] was recorded at 300 K with 16 scans, 512 experiments of 1024 data points, a sweep width of 4000 Hz in f_2 and 17857 Hz in f_1 with GARP decoupling (90° = 72 μs) during the acquisition. The relaxation delay (225 ms) and recovery delay after BIRD (198 ms) were optimized to minimize the signal obtained after 2 dummy scans. Zero-filling in f_1 and phase-sensitive processing yielded a final data matrix of 1024 × 2048.

The HMQC experiment without the BIRD scheme was recorded at 243 K with a relaxation delay of 1.1 s. The remaining parameters were the same as defined for the HMQC experiment with BIRD. The HMQC with TOCSY transfer was recorded at 300 K with an MLEV17 [30] mixing sequence of 80 ms and spin-locking field strength of 8.9 Hz.

The DEPT-HMQC spectra [36] were recorded at 300 K with 16 scans of 1024 data points, 512 experiments, a spectral width of 4000 Hz in f_2 and 17857 Hz in f_1, a relaxation delay of 225 ms and GARP decoupling during acquisition. The signal from the BIRD sequence was minimized with a recovery delay of 198 ms. The DEPT proton pulse was π to produce positive CH and CH_3 and negative CH_2 signals. The experimental data matrix was zero-filled to 2048 × 1024 complex points. A shifted sinebell apodization in f_2 and exponential 5-Hz line broadening in f_1 were applied before the phase-sensitive *Fourier* transformation.

The HSQC [37] experiment (often referred to as *OverBodenhausen*) with TOCSY was recorded at 300 K with 64 scans, 512 experiments of 1024 data points, and a sweep width of 4000 Hz in f_2 and 17857 Hz in f_1 with GARP decoupling during the acquisition. The spin lock mixing of 100 ms was achieved with the MLEV17 sequence. Zero filling in f_1 and phase sensitive processing yielded a final data matrix of 2048 × 2048.

The 3D HQQC-TOCSY [38] experiment was recorded at 300 K with 48 scans, 1024 data points and 64 and 90 experiments, in t_1 and t_2, resp., and a sweep width of 4000 Hz in f_3, 1562 Hz in f_2, and 1712 Hz in f_1.

To obtain the heteronuclear coupling constants, a 3D HMQC-TOCSY without decoupling with extensive folding was carried out at 300 K with 64 scans, 1024 data points and 64 and 128 experiments, in t_1 and t_2, resp., and a sweep width of 4000 Hz in f_3, 3012 Hz in f_2 and 3289 Hz in f_1. A full description of this experiment will appear elsewhere [39].

Computer Simulations. The molecular-dynamics (MD) simulations were carried out with the Discover (BIOSYM) program [40]. The X-ray structure of FK506 (**2**) from the *Cambridge Data Bank* [5] was used to build the molecular structure and topology. The parameters for the energetic description of the tricarbonyl hemiacetal portion of the molecule are undefined in commonly utilized force fields [41]. For these undefined parameters, the equilibrium values were set to those from the X-ray structure, and the force constants approximated from standard literature values of related structures. For the force constant of the torsion between the two carbonyl groups (N(7)–C(8)–C(9)–C(10)), two separate test MD simulations were carried out, with force constants of 20.0 and 0 kcal/mol. From these simulations (details described below), no significant differences were observed and,

therefore, the force constant of 20.0 kcal/mol was utilized for all further calculations. All computer simulations were carried out *in vacuo* on *Silicon Graphics 4D/240SX* and *4D/70GTB* computers.

The distance restraints were derived from the NOE's with a two-spin approximation using the NOE's between geminal protons and a distance of 1.78 Å as a reference. The upper and lower distance bounds were set to plus and minus 5% of the calculated distances. This small variation allows for some error in the measurement of the intensity of cross-peaks and the conversion to distances. The application of the NOE's was modified from our previous simulation [28]. Restraints to Me group protons now use the C-atom with the addition of 0.3 Å to the upper bound [42]. In addition, all distance restraints with diastereotopic methylene protons take now into account their configurational assignments. These modifications were necessary to avoid the use of proton restraints to the average position of a group of protons (methylene or methyl).

The NOE-restrained MD simulations were carried out with a time step of 1.0 fs for a duration of 100 ps. The atomic velocities were randomly applied following a *Boltzmann* distribution about the center of mass to obtain a temp. of 1000 K. The observed NOE restraints were then introduced using a relatively high force constant (a maximum force of 1000 kcal/mol·Å^2), and the system was allowed to come to equilibrium for 10 ps. A skewed biharmonic constraining function was used for the NOE restraints. The temp. was then reduced to 500 K and the NOE force constants reduced: Maximum forces of 200 and 40 kcal/mol·Å^2 were used for the lower and upper distance restraints, respectively. The use of a maximum force produces a linear function when there is a large difference between the target and actual distances. During the MD, structures were taken at regular intervals and completely energy-minimized using a quasi *Newton-Raphson* minimizer [43] until the derivatives were less then 0.005 kcal/mol·Å.

The X-ray structure of **2** was used as the starting conformation for the simulation of the *cis*-isomer (major). The starting structure of the *trans*-isomer (minor) was generated by application of dihedral forcing potentials and subsequent energy minimization: the torsion O(1)–C(1)–C(2)–C(3) and C(2)–N(7)–C(8)–C(9) (omega bond) were forced to 119 and 180°, resp., while all other torsions were forced to the values found in the X-ray structure of **2**. This method is different from that employed in our previous study [28] where only the 'omega' torsion was modified (from *cis* to *trans*) with a forcing potential. This process indeed produced a *trans* omega bond, but also caused the torsion C(8)–C(9)–C(10)–C(11) to change by 180°. In the X-ray structure of rapamycin (**3**) which contains a *trans* omega bond, it is the O(1)–C(1)–C(2)–C(3) torsion that changes by 180° (with respect to **2**) to account for the change in the omega torsion. All other torsions within this region are very similar in the X-ray structures of **2** and **3**. Therefore, to create the starting structure for the *trans-isomer* (minor), we have chosen to force the O(1)–C(1)–C(2)–C(3) and omega torsions to the values found in the solid-state structure of **3** and all other torsions to those found for **2**.

Results and Discussion. – *Assignment of the NMR Spectra.* For an unambiguous interpretation of the NOE data, the complete assignment of the ^{1}H-NMR spectrum is an absolute prerequisite. However, even at 600 MHz, the ^{1}H-NMR spectrum of FK506 (**2**) displayed severe spectral overlap (see *Fig. 1a*). Especially problematic is the close similarity of the chemical shifts of the corresponding protons of the two conformations, illustrated in the TOCSY spectrum shown in *Fig. 2*. In the ^{13}C-NMR spectrum (*Fig. 1b*), the overlap is much less severe, and thus it was clear that heteronuclear spectra would be of great importance during the assignment procedure (an HMQC is shown in *Fig. 3*).

The assignment was achieved using a variety of homonuclear (DQF-COSY, TOCSY, ROESY) and heteronuclear (HMQC, DEPT-HMQC, HSQC with TOCSY transfer, HMBC) two-dimensional techniques and was confirmed with the powerful three-dimensional HQQC-TOCSY. To achieve configurational assignments and extract homonuclear and heteronuclear coupling constants, an E. COSY and a three-dimensional HMQC-TOCSY without heteronuclear decoupling [44] were recorded.

The ^{1}H-NMR spectrum of **2** exhibits five spin systems interrupted by quaternary C-atoms (C*H*(2) to C*H*$_2$(6), C*H*$_3$(35) to C*H*$_2$(18), C*H*(20) to C*H*$_2$(40), C*H*$_2$(23) to C*H*(26), C*H*(28) to C*H*$_2$(34)) and several isolated Me groups (C*H*$_3$(37), C*H*$_3$(42) to C*H*$_3$(45)). To avoid any circular arguments, the assignment was accomplished with the exclusive utilization of through-bond couplings.

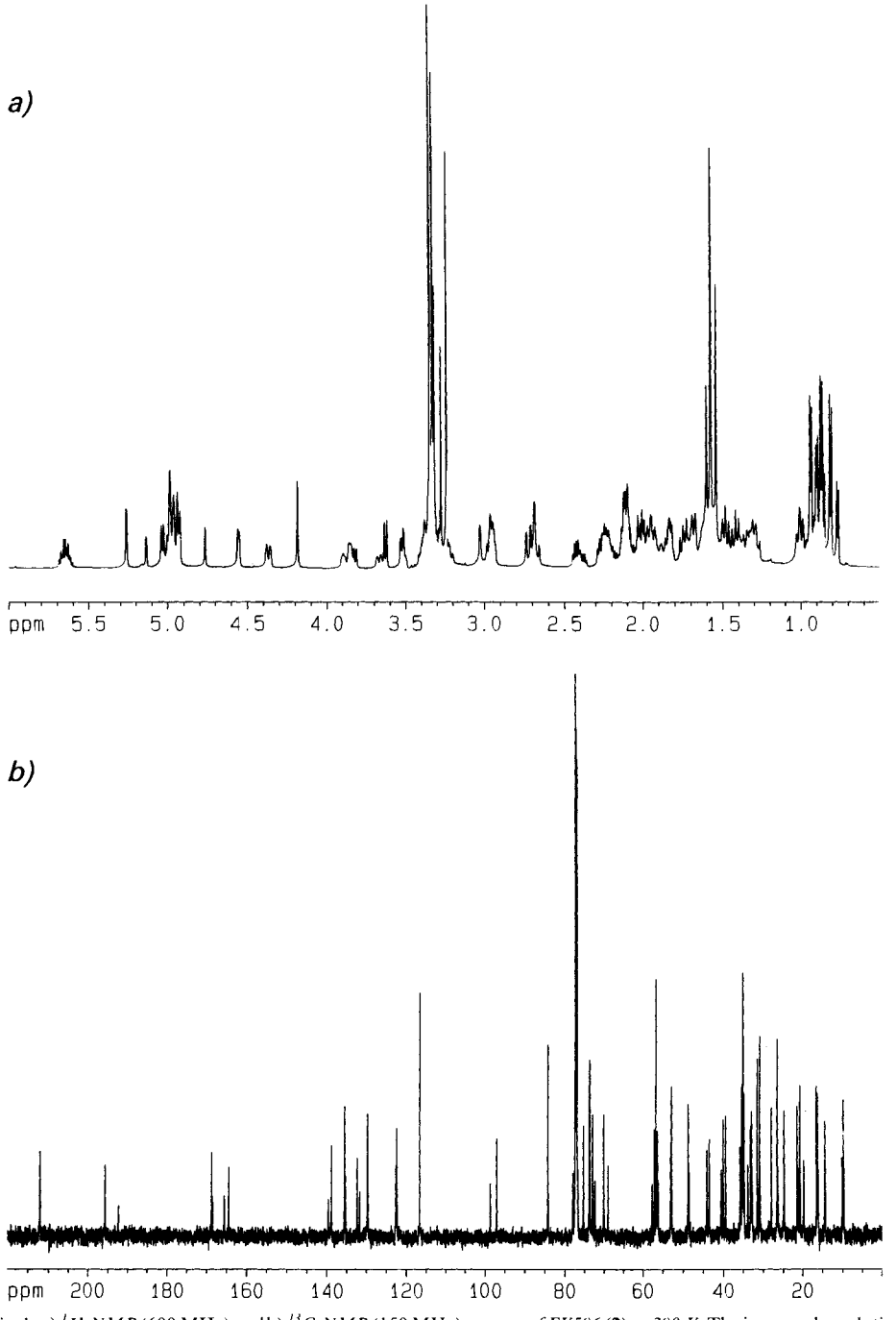

Fig. 1. a) *^{1}H-NMR* (600 MHz) *and* b) *^{13}C-NMR* (150 MHz) *spectra of FK506* (**2**) *at 300 K*. The increased resolution of the ^{13}C-NMR spectrum is clearly visible, with even the most similar C-atoms from the two conformations well resolved.

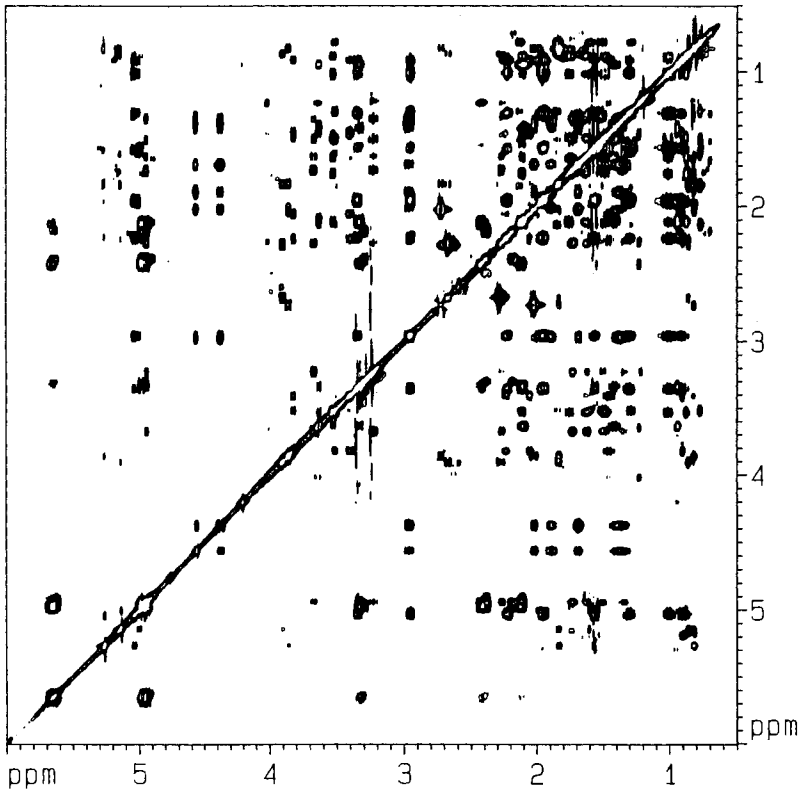

Fig. 2. *2D-TOCSY of FK506* (**2**). Recorded at 500 MHz and 300 K using the MLEV-17 mixing sequence for 100 ms.

The assignment procedure started at CH_2(40), whose ^{1}H-NMR signal was the only methylene group at low field, as can easily be seen in the DEPT-HMQC (*Fig. 4*). The DQF-COSY and TOCSY experiments, always supported by heteronuclear correlations, were used to assign the spin system from CH_2(40) to CH(20). Since in olefinic compounds of this type, the homonuclear four-bond coupling constants can be of considerable size, a correlation of CH(20) to CH_3(37) was found in the TOCSY; CH_3(37) in turn is connected to CH_2(18) by a correlation in the ROESY. However, less ambiguous is a correlation in the HMBC, in this case, the correlation from CH_2(18) to C(20) (see *Fig. 5b*). From CH_2(18), the spin system to CH_3(35) was assigned again by a combination of homonuclear and heteronuclear techniques. The same methods were employed for the other spin systems, always confirming the assignments with correlations in the HMBC. The different isolated Me groups were also identified in the HMBC by their correlations *via* two- and/or three-bond couplings (*Fig. 5*). The same is true for the quaternary C-atoms (C(1), C(8) to C(10), C(19), C(27)).

Since the Me groups CH_3(35), CH_3(36), and CH_3(41) are distributed in two of the five spin systems, the assignments could be confirmed with the three-dimensional HQQC-TOCSY experiment, which selects Me groups in a heteronuclear correlation and is extended with a TOCSY transfer. The execution of a three-dimensional experiment with

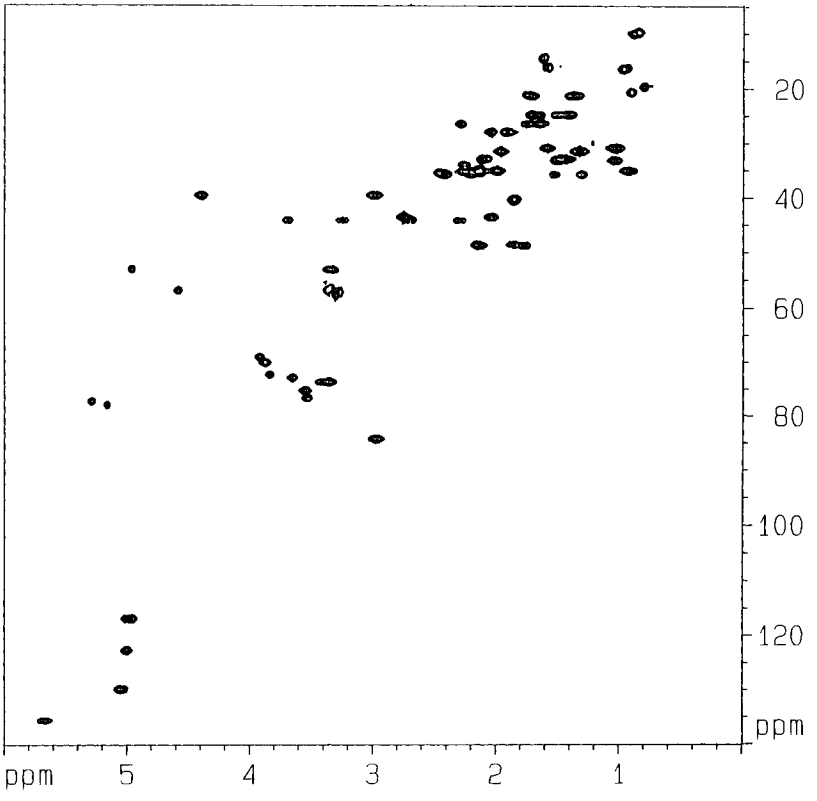

Fig. 3. *2D-HMQC of FK506* (**2**). Recorded at 500 MHz and 300 K.

a molecule of this size is not 'overkill', since it has been demonstrated previously that very informative spectra of molecules with the heteronucleus in natural abundance can be performed in a rather short time [45]. Slices of the 3D HQQC-TOCSY of FK506 (**2**), with a total measuring time of only 32 h, are shown in *Fig. 6*. The high resolution from the relatively long measuring time for this type of experiments is obvious and greatly simplified the assignment procedure. The complete ^{1}H- and ^{13}C-assignments of FK506 (**2**) in $CDCl_3$ are given in *Table 1*.

The assignment of the individual diastereotopic methylene protons was particularly difficult: the homonuclear coupling constants in conjunction with NOE effects, often used in proteins, are not sufficient to allow unambiguous assignments. Hence, it was necessary to define the ^{3}J(C,H) coupling constants of both diastereotopic protons and use these values in conjunction with ^{3}J(C,H) to define the conformation of the ethane fragments. For the determination of heteronuclear coupling constants, the relatively low concentration and severe spectral overlap necessitated a sensitive method allowing good resolution. Two methods for the quantitative determination of heteronuclear coupling constants usually fulfill these demands; the method of *Titman* and *Keeler* [46] and the method of *Montelione et al.* [47]. The former seems to be the best method available to measure couplings to quaternary C-atoms, but the technique suffers from the extremely

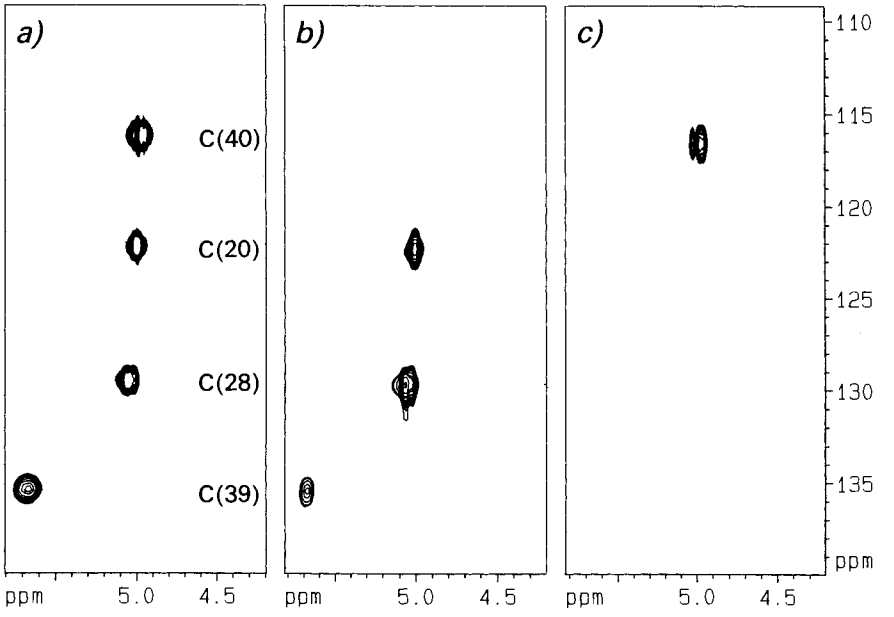

Fig. 4. *Comparison of the olefinic region in the HMQC and the DEPT-HMQC of FK506* (**2**): a) *HMQC*, b) *positive levels in the DEPT-HMQC, and* c) *negative levels in the DEPT-HMQC*. Recorded at 500 MHz and 300 K. The assignment of CH_2(40) is straightforward, since it is the only methylene group in the olefinic region.

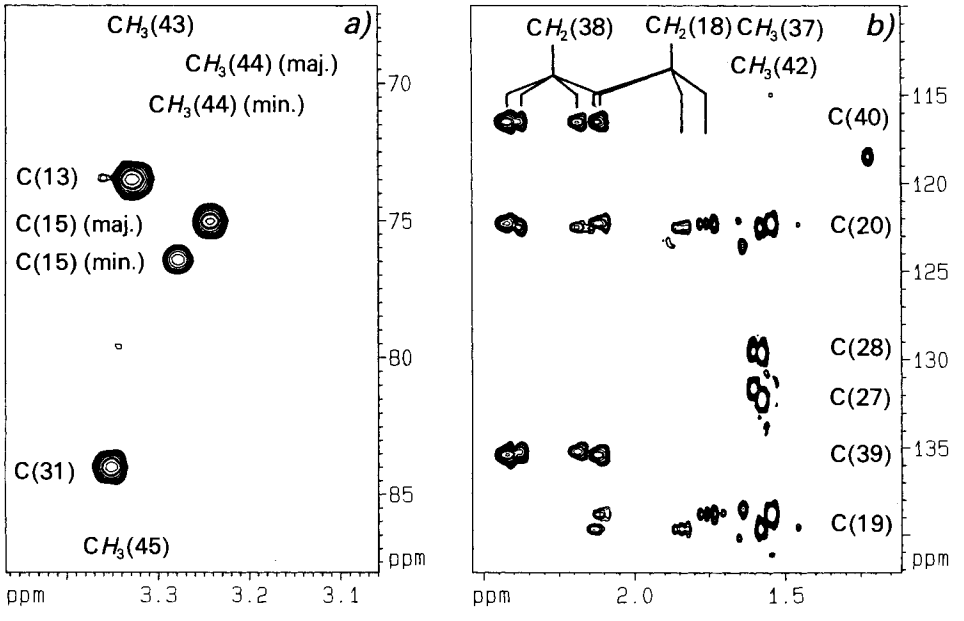

Fig. 5. *Selected regions of the HMBC* (600 MHz, 300 K) *of FK506* (**2**): a) *Region of the correlations between the protons of the MeO groups and the C-atoms three bonds away* (unambiguous identification of the different MeO groups). b) *Connection of the spin systems from* CH_2*(40) to* CH*(20) and from* CH_2*(18) to* CH_3*(35)*. The correlation from CH_2(18) to C(20) establishes the connection of both spin systems over the quaternary C(19). In addition, the identification of CH_3(37) and CH_3(42) is visible.

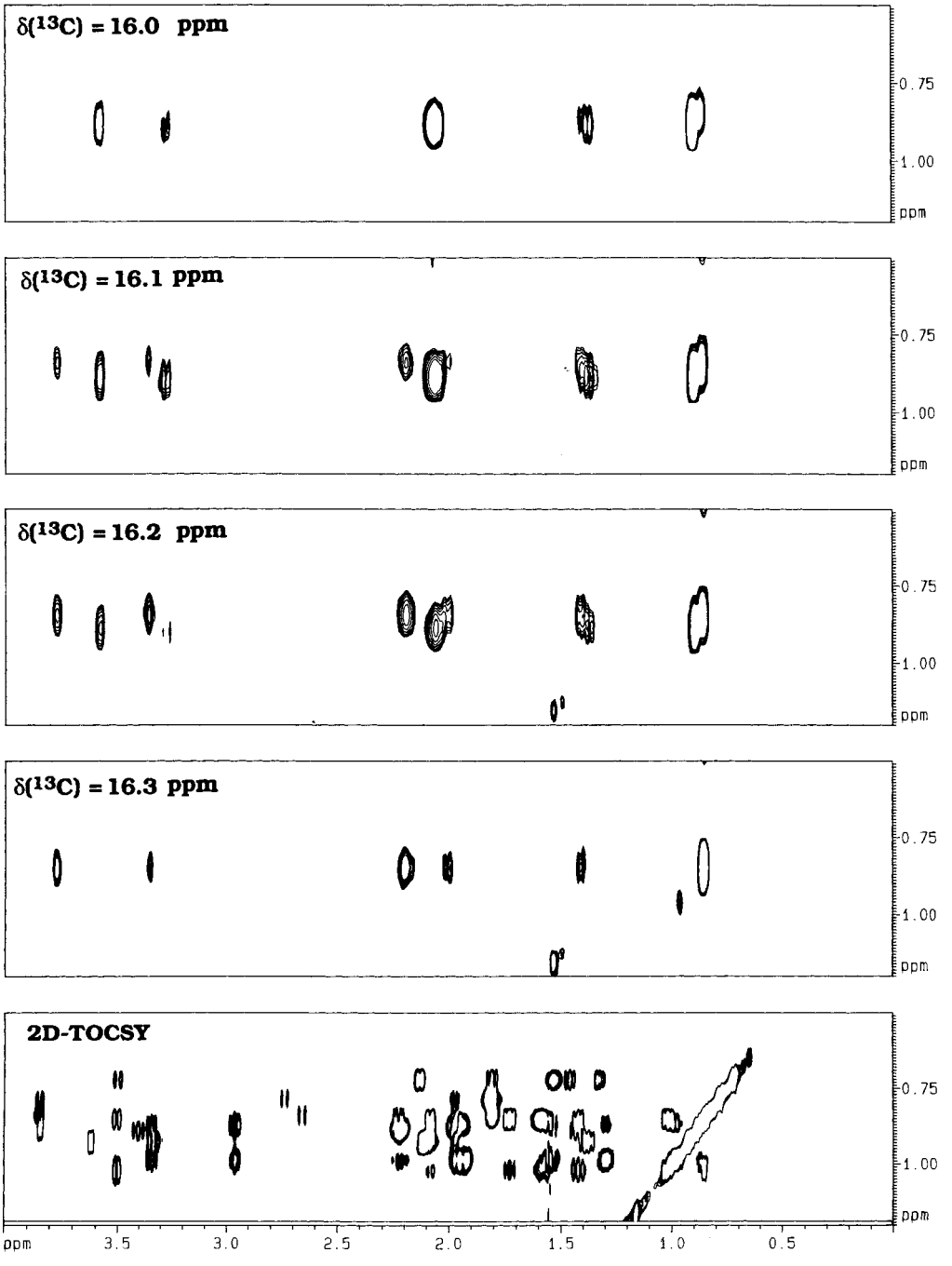

Fig. 6. *Adjacent slices from the 3D-HQQC-TOCSY of FK506* (**2**). Recorded at 500 MHz and 300 K. The slices show the resonances at the ^{13}C frequencies of C(35). By progressing from slice to slice, the two conformations can be separated and their correlations independently confirmed.

Table 1. *Chemical Shifts* δ [ppm] *of FK506* (**2**) *in* $CDCl_3$ *at 243 K*[a])

	Major isomer (*trans*)		Minor isomer (*cis*)	
	δ(C)	δ(H)	δ(C)	δ(H)
C(1)	168.95	–	168.68	–
CH(2)	56.55	4.53	52.69	4.94
CH_2(3)	27.67	1.83(ax), 2.02(eq)	26.21	1.73(ax), 2.31(eq)
CH_2(4)	21.12	1.28(ax), 1.69(eq)	20.83	1.25(ax), 1.74(eq)
CH_2(5)	24.51	1.41(ax), 1.69(eq)	24.56	1.47(ax), 1.63(eq)
CH_2(6)	39.22	2.98(ax), 4.36(eq)	43.85	3.14(ax), 3.68(eq)
C(8)	164.63	–	165.78	–
C(9)	196.11	–	192.57	–
C(10)	97.00	–	98.63	–
CH(11)	34.56	2.10 (OH at 4.23)	33.62	2.22 (OH at 4.86)
CH_2(12)	32.69	1.39(ax), 2.12(eq)	32.55	1.43(ax), 2.07(eq)
CH(13)	73.52	3.33	73.50	3.41
CH(14)	72.78	3.63	72.21	3.83
CH(15)	75.14	3.51	76.54	3.50
CH_2(16)	32.91	1.02 (*pro-R*), 1.42 (*pro-S*)	35.44	1.33 (*pro-R*), 1.46 (*pro-S*)
CH(17)	26.21	1.59	26.02	1.53
CH_2(18)	48.54	1.73 (*pro-R*), 2.09 (*pro-S*)	48.35	1.81 (*pro-S*), 2.13 (*pro-R*)
C(19)	138.94	–	139.81	–
CH(20)	122.42	4.93	122.65	4.94
CH(21)	52.74	3.33	52.89	3.30
C(22)	212.68	–	212.56	–
CH_2(23)	43.21	1.98 (*pro-S*), 2.74 (*pro-R*)	43.85	2.23 (*pro-S*), 2.67 (*pro-R*)
CH(24)	69.99	3.85	68.89	3.86
CH(25)	39.82	1.82	40.40	1.80
CH(26)	77.13	5.27	77.85	5.10
C(27)	132.39	–	131.75	–
CH(28)	129.66	5.01	129.70	4.94
CH(29)	34.86	2.23	34.89	2.22
CH_2(30)	34.83	0.88(ax), 1.97(eq)	34.74	0.88(ax), 1.99(eq)
CH(31)	84.15	2.97	84.15	2.96
CH(32)	73.63	3.35	73.61	3.35
CH_2(33)	31.20	1.29(ax), 1.93(eq)	31.18	1.27(ax), 1.93(eq)
CH_2(34)	30.61	0.99(ax), 1.56(eq)	30.61	0.98(ax), 1.55 (eq)
CH_3(35)	16.23	0.93	16.00	0.89
CH_3(36)	20.41	0.86	19.41	0.72
CH_3(37)	15.96	1.52	15.78	1.55
CH_2(38)	35.11	2.12, 2.41	35.55	2.22, 2.36
CH(39)	135.54	5.64	135.33	5.62
CH_2(40)	116.66	4.93, 4.98	116.66	4.95, 4.98
CH_3(41)	9.48	0.79	9.80	0.85
CH_3(42)	14.10	1.55	14.23	1.59
CH_3(43)	56.29	3.34	56.08	3.33
CH_3(44)	56.97	3.24	57.55	3.30
CH_3(45)	56.58	3.35	56.58	3.35

[a]) The numbering of the heavy atoms is from *Cambridge Data Bank* coordinate file.

Table 2. *Heteronuclear Coupling Constants J(C,H)* [Hz] *of the Major and Minor Isomers of FK506* (**2**), *Determined from a 3D-HMQC-TOCSY*[a])

C-Atom	H-Atom	J[b])		C-Atom	H-Atom	J[b])	
		Major isomer (*trans*)	Minor isomer (*cis*)			Major isomer (*trans*)	Minor isomer (*cis*)
C(2)	H–C(6)	0.0	0.4	C(16)	H–C(18)	2.5	1.7
	H′–C(6)	3.8	4.5	(cont.)	H′–C(18)	6.8	1.6
	H–C(5)	–	0.0		CH_3(36)	2.5	2.9
	H′–C(5)	–	0.0	C(17)	CH_3(36)	–4.0	–3.5
	2 H–C(4)	–	4.2	C(18)	CH_3(36)	4.6	3.4
	H–C(3)	–4.8	–	C(20)	CH_3(37)	4.6	5.0
	H′–C(3)	–2.0	–1.1		H–C(38)	1.6	4.3
C(3)	H–C(6)	0.0	0.0		H′–C(38)	5.5	3.5
	H′–C(6)	0.0	0.0		H–C(39)	0.0	–
	H–C(5)	2.0	3.6	C(23)	H–C(24)	–2.0	–1.1
	H′–C(5)	–	5.7		H–C(25)	–	5.2
	H–C(4)	–2.3	–4.0		CH_3(41)	0.0	0.0
	H′–C(4)	–	–2.3	C(24)	H–C(23)	–6.8	–6.1
	H–C(2)	–3.6	–3.5		H′–C(23)	–1.8	–1.3
C(4)	H–C(6)	1.0	1.7		H–C(25)	–5.5	–4.1
	H′–C(6)	4.9	7.1		H–C(26)	1.7	3.0
	H′–C(3)	–2.5	–2.9		CH_3(41)	4.2	4.0
	H–C(2)	4.5	5.3	C(25)	H–C(23)	–	4.7
C(5)	H–C(6)	–3.8	–1.1		H′–C(23)	2.4	1.0
	H′–C(6)	–1.4	–3.9		H–C(24)	–2.2	–1.7
	H–C(3)	2.8	–		H–C(26)	–2.4	–2.5
	H′–C(3)	5.8	5.9		CH_3(41)	–3.7	–4.2
	H–C(2)	0.5	0.0	C(26)	H–C(25)	–4.4	0.0
C(6)	H–C(5)	–	4.8		CH_3(41)	3.9	4.4
	H′–C(5)	–	–2.7		CH_3(42)	5.2	4.8
	H–C(4)	–	3.6	C(35)	H–C(11)	–	–3.3
	H′–C(4)	–	5.7		2 H–C(12)	3.9	2.3
	H–C(3)	0.0	0.0		H–C(13)	0.0	0.0
	H′–C(3)	0.0	–		H–C(14)	0.0	0.0
	H–C(2)	2.8	3.1	C(36)	H–C(15)	0.0	0.0
C(12)	H–C(13)	–	–1.3		H–C(16)	–	2.8
	H–C(14)	2.3	0.8		H′–C(16)	7.6	5.5
	CH_3(35)	3.6	3.0		H–C(17)	–4.2	–2.4
C(13)	H–C(14)	–3.7	–4.4		H–C(18)	3.0	3.1
C(14)	H–C(13)	–3.9	–4.7		H′–C(18)	3.3	7.5
	H–C(12)	2.3	2.2	C(37)	H–C(20)	7.8	–
	H′–C(12)	–	6.0	C(41)	H–C(23)	0.0	0.0
	H–C(11)	–	0.0		H′–C(23)	0.0	0.0
	CH_3(35)	0.0	0.0		H–C(24)	1.9	2.2
C(15)	H–C(16)	–6.0	–6.4		H–C(25)	–3.5	–3.9
	H′–C(16)	–5.6	–5.3		H–C(26)	3.5	4.0
	H–C(17)	3.5	5.5	C(42)	H–C(26)	3.3	3.3
	H′–C(18)	0.0	–		H–C(28)	8.2	8.5
	CH_3(36)	0.0	0.0	C(40)	H–C(38)	5.5	6.8
C(16)	H–C(15)	–2.5	–3.3		H′–C(38)	6.4	4.4
	H–C(17)	–2.0	–		H–C(39)	0.0	–

[a]) The prime (′) indicates low-field proton.

[b]) Where no coupling constant is given, the value could not be determined because of overlap or weakness of the correlation in the TOCSY.

Table 3. *Heteronuclear Coupling Constants* J(*C,H*) [Hz] *of the Exocyclic Portion of FK506* (**2**). The higher mobility results in only one set of signals at 300 K[a]).

C-Atom	H-Atom	*J*	C-Atom	H-Atom	*J*
C(28)	H–C(29)	–3.0	C(32)	H–C(34)	2.1
	2 H–C(30)	2.0		H′–C(34)	5.0
	H–C(31)	0.8	C(33)	H–C(28)	0.0
	H–C(32)	0.0		H–C(29)	1.2
	2 H–C(33)	0.0		2 H–C(30)	0.0
	H–C(34)	3.9		H–C(31)	1.5
	H′–C(34)	4.2		H–C(32)	–4.4
C(30)	H–C(28)	0.8		H–C(34)	–3.7
	H–C(29)	–3.7		H′–C(34)	–2.5
	H–C(31)	0.0	C(34)	H–C(28)	4.1
	H–C(33)	0.0		H–C(29)	–4.6
	H′–C(33)	0.0		2 H–C(30)	4.1
	H′–C(34)	2.4		H–C(31)	0.0
C(31)	H–C(28)	0.0		H–C(32)	0.0
	H–C(29)	0.7		2 H–C(33)	–2.8
	2 H–C(30)	–6.8			
	H–C(32)	–4.8			
	2 H–C(33)	2.6			
	H–C(34)	–0.5			
	H′–C(34)	–0.5			

[a]) The prime (′) indicates low-field proton. Where no coupling constant is given, the value could not be determined because of overlap or weakness of the correlation in the TOCSY.

long time that would have been necessary to obtain an HMBC of sufficient intensity and the problems with the extraction of a reference *multiplet* from either the TOCSY or heteronuclear spectrum because of the spectral overlap. For heteroatoms with directly attached protons, the latter technique is superior as the interesting long-range coupling appears in t_2 as in-phase displacements in E. COSY-type patterns, and the pulse sequence is generally shorter. For FK506 (**2**), the most important coupling constants involve the C-atom of Me groups, their long-range couplings allowing for the assignment of the diastereotopic protons of the adjacent methylene groups. Thus, the latter technique, in this case with a TOCSY as the homonuclear experiment, is especially advantageous since the correlation from the Me protons to other protons are usually very intense in a TOCSY, whereas correlations to Me C-atoms in an HMBC are much weaker. It had, however, to be executed as a three-dimensional technique because of the extreme overlap in the two-dimensional TOCSY, that would have been even worse from the doubling of the signals with this technique (*i.e.* no decoupling). A detailed description of the experiment will be given elsewhere [39]. The coupling constants obtained from these experiments are listed in *Tables 2* and *3*. The homonuclear and heteronuclear three-bond coupling constants necessary for the assignments of the diastereotopic protons at C(16), C(18), and C(23) are given in *Table 4*.

The assignment of the 2 H–C(18) is straightforward for both the major and minor isomers. The fact of having two heteronuclear coupling constants doubly confirms these assignments. For the 2 H–C(16), overlapping resonances do not allow the measurement of all coupling constants. For the major isomer, the assumption that the extremely large (7.6 Hz) ^3J(C(36),*H*–C(16)) indicates a *trans*-orientation of these two (looking down the C(16)–C(17) bond) and, therefore, a *gauche* orientation of C(36) and *H*′–C(16) (low field) was adopted. A similar

Table 4. *$^3J(H,H)$ and $^3J(C,H)$ Coupling Constants* [Hz] *of the Major and Minor Isomers of FK506* (**2**) *Used for the Assignment of the Diastereotopic Methylene Protons at C(16), C(18), and C(23)*[a])

		J	
		Major isomer	Minor isomer
CH_2(16)	*H*–C(16), *H*–C(17)	10.8	9.3
	H'–C(16), *H*–C(17)	5.5	[b])
	C(36), *H*–C(16)	[b])	2.8
	C(36), *H'*–C(16)	7.6	5.5
	Assignment	H–C(16) *pro-R*	H–C(16) *pro-R*
		H'–C(16) *pro-S*	H'–C(16) *pro-S*
CH_2(18)	*H*–C(18), *H*–C(17)	10.8	9.3
	H'–C(18), *H*–C(17)	5.5	5.8
	C(16), *H*–C(18)	2.5	1.7
	C(16), *H'*–C(18)	6.8	1.8
	C(36), *H*–C(18)	3.0	3.1
	C(36), *H'*–C(18)	3.3	7.5
	Assignment	H–C(18) *pro-R*	H–C(18) *pro-S*
		H'–C(18) *pro-S*	H'–C(18) *pro-R*
CH_2(23)	*H*–C(23), *H*–C(24)	3.4	2.3
	H'–C(23), H–C(24)	9.2	8.9
	C(25), H–C(23)	[c])	4.7
	C(25), H'–C(23)	2.4	1.0
	Assignment	H–C(23) *pro-S*[d])	H–C(23) *pro-S*
		H'–C(23) *pro-R*	H'–C(23) *pro-R*

[a]) The prime (') indicates low-field proton.
[b]) Coupling constant was not measured because of overlapping resonances.
[c]) Intensity was too weak for accurate measurement of coupling constant.
[d]) The assignment of the 2 H–C(23) of the major isomer was obtained from the assignment of the 2 H–C(23) of the minor isomer and exchange cross-peaks in NOESY and ROESY experiments.

assumption was used for the 2 H–C(16) of the less populated minor isomer. Here, the homonuclear coupling between *H*–C(16) (high field) and *H*–C(17) could not be determined. However, the relatively large value for *H'*–C(16) (low field) indicates a *trans* orientation (looking down the C(16)–C(17) bond), and, therefore, *H*–C(16) (high field) and *H*–C(17) must have a *gauche* orientation. The assigments of prochirality to the 2 H–C(16) following these arguments are given in *Table 4*.

The 2 H–C(23) of the major isomer cannot be unambiguously identified from the coupling constants. The *J*(*H'*–C(23),*H*–C(24)) and *J*(*H*–C(23),*H*–C(24)) indicate a *trans* and *gauche* orientation for *H'*–C(23) (low field) and *H*–C(23) (high field), respectively, but the heteronuclear coupling constant with C(25) could only be measured for the high-field proton *H*–C(23). On the other hand, for the minor isomer, both ^3J(C,H) were measured, and the assignment was possible (*Table 4*). However, since the two isomers are undergoing exchange (as seen from the ROESY and NOESY), the assignment of prochirality for the major isomer can be made from the assignment of the minor isomer (*i.e.* the *pro-R* proton of the minor isomer will only show exchange peaks to the *pro-R* proton of the major isomer). And indeed, there are exchange peaks between the high-field protons of the two isomers (indicating that both are *pro-S*) and low-field protons (both are *pro-R*). Similar analysis of the exchange peaks observed for the 2 H–C(16) and the 2 H–C(18) is in agreement with the configurational assignments based on the coupling constants. This can be thought of as an additional proof of the prochirality assignments.

Conformational Analysis. Besides the assignment of the diastereotopic methylene protons, coupling constants were used to determine rotamer populations of dihedral angles. The conformationally informative coupling constants are listed in *Table 5*. Using the assignment of the diastereotopic CH_2(16) protons, the preferred conformation of the C(15)–C(16) torsion can be calculated from the homonuclear ^3J(H,H) with *H*–C(15).

Table 5. $^3J(H,H)$ *and* $^3J(C,H)$ *Coupling Constants* [Hz] *Used in the Conformational Analysis of the Major an Minor Isomers of FK506* (**2**)[a])

	Coupling	Bond[b])	J		Angle[c])
			Major isomer	Minor isomer	
^3J	H–C(15), H–C(16)	C(15)–C(16)	4.8	3.8	
	H–C(15), H'–C(16)		11.0	10.6	
^3J	H–C(24), H–C(25)	C(24)–C(25)	[d])	[d])	
	C(23), H–C(25)		[e])	5.1	
	C(41), H–C(24)		1.9	2.2	
^3J	H–C(25), H–C(26)	C(25)–C(26)	10.3	9.9	180°
	C(24), H–C(26)		1.7	3.0	
	C(41), H–C(26)		3.5	4.0	
^3J	H–C(21), H–C(38)	C(21)–C(38)	7.5[f])	7.5[f])	60°
	H–C(21), H'–C(38)		8.0[f])	8.0[f])	
	C(20), H–C(38)		1.6	4.3	
	C(20), H–C(38)		5.5	3.5[g])	
^2J	H–C(23), H'–C(23)	C(22)–C(23)	15.8	17.4	*ca.* 0°

[a]) The prime (') indicates low-field proton.
[b]) C(15)–C(16) for C(14)–C(15)–C(16)–C(17); C(24)–C(25) for C(23)–C(24)–C(25)–C(26); C(25)–C(26) for C(24)–C(25)–C(26)–C(27); C(21)–C(38) for C(20)–C(21)–C(38)–C(39); C(22)–C(23) for C(21)–C(22)–C(23)–C(24).
[c]) Torsion predicted from coupling constants.
[d]) Coupling constant was not measured because of overlapping resonances.
[e]) Intensity was too weak for accurate measurement of coupling constant.
[f]) Coupling constant estimated from a three-spin E. COSY.
[g]) Large deviation in measured coupling constant.

The large coupling constant (11.0 and 10.6 Hz, major and minor isomers, resp.) for H–C(16) (high field) indicates a *trans* orientation, while the small values (4.8 and 3.8 Hz, major and minor isomers, resp.) for H'–C(16) (low field) indicates a *gauche* orientation. The resulting heavy-atom torsion (C(14)–C(15)–C(16)–C(17)) is *gauche* positive (+60°).

The torsion about the C(25)–C(26) bond can be estimated from the two heteronuclear ^3J(C(24),H–C(26)) and ^3J(C(41),H–C(26)) and the homonuclear ^3J(H–C(25), H–C(26)) (see *Table 5*). The large ^3J(H,H) and equal values for the heteronuclear coupling constants suggest a rotamer having an angle of 180° for the heavy-atom torsion C(24)–C(25)–C(26)–C(27).

The C(20)–C(21)–C(38)–C(39) torsion can be estimated from the heteronuclear ^3J(C(20),H–C(38)) and the homonuclear ^3J(H–C(21),H–C(38)). The homonuclear coupling constants were estimated from the E. COSY spectrum carried out for three spins. The pattern of the cross-peak is complicated because of the couplings to H–C(20) and H–C(39). However, exploiting the higher proton multiquantum coherences (greater than four) in the E. COSY experiment is complicated by low sensitivity and instrumental difficulties. Nevertheless, it is possible to extract coupling constants for the spin system mentioned above by the analysis of the fine structure of cross-peaks in the three-spin E. COSY spectrum. From the coupling constants listed in *Table 5*, the torsion angle is estimated to be 60° for both isomers.

The coupling constant between geminal protons are of little conformational value for most parts. However, when adjacent to carbonyl groups and the carbonyl subtends the

geminal protons, the overlapping of the p-orbitals of the carbonyl causes a great increase in the ^2J coupling constant of the protons. Following this reasoning, the large geminal coupling ^2J(H–C(23),*H'*–C(23)) of 17.4 Hz of the minor isomer indicates that the carbonyl group of C(22) is *gauche* to both H–C(23) and H'–C(23). This leads to a C(21)–C(22)–C(23)–C(24) torsion angle of close to zero.

The unambiguously assigned NOE's are listed in *Table 6*. The distances shown were calculated from a comparison with the volume of the NOE's from geminal protons with

Table 6. *Calculated H–H Distances* [Å] *from Experimentally Measured NOE's at 243 K in $CDCl_3$ of the Major and Minor Isomers of FK506* (**2**)[a])

Atoms		Distance		Atoms		Distance	
		Major isomer	Minor isomer			Major isomer	Minor isomer
H–C(2)	H_{ax}–C(3)	2.3	2.5	$H_{pro\text{-}R}$–C(16)	$H_{pro\text{-}S}$–C(18)	3.2	
H–C(2)	H_{eq}–C(3)	2.3		$H_{pro\text{-}R}$–C(16)	$H_{pro\text{-}R}$–C(18)	3.4	
H–C(2)	$H_{pro\text{-}S}$–C(16)	2.8		$H_{pro\text{-}R}$–C(16)	Me(36)		2.9
H–C(2)	$H_{pro\text{-}R}$–C(18)	3.9		$H_{pro\text{-}R}$–C(16)	Me(44)	2.6	3.3
H–C(2)	$H_{pro\text{-}R}$–C(23)	5.0		$H_{pro\text{-}S}$–C(16)	Me(44)	4.7	
H_{ax}–C(3)	H_{ax}–C(4)	2.9		*H*–C(17)	$H_{pro\text{-}R}$–C(18)	2.7	
H_{ax}–C(3)	H_{eq}–C(4)	2.7		$H_{pro\text{-}R}$–C(18)	*H*–C(20)	2.6	2.6
H_{ax}–C(3)	*H*–C(28)	2.7		$H_{pro\text{-}S}$–C(18)	*H*–C(20)	2.3	2.3
H_{ax}–C(3)	Me(44)	3.9		$H_{pro\text{-}R}$–C(18)	Me(36)	2.9	
H_{ax}–C(4)	H_{ax}–C(6)		4.0	$H_{pro\text{-}S}$–C(18)	Me(36)		3.7
H_{ax}–C(4)	H_{eq}–C(6)	4.9		$H_{pro\text{-}S}$–C(18)	Me(37)		2.6
H_{ax}–C(4)	*H*–C(28)	3.3		*H*–C(20)	$H_{pro\text{-}R}$–C(23)	4.0	4.4
H_{eq}–C(4)	*H*–C(28)		3.3	*H*–C(21)	Me (37)	2.4	2.5
H_{ax}–C(5)	H_{ax}–C(6)	3.5		$H_{pro\text{-}R}$–C(23)	*H*–C(25)	3.7	4.3
H_{ax}–C(5)	H_{eq}–C(6)	2.5		$H_{pro\text{-}R}$–C(23)	*H*–C(26)	3.4	2.9
H_{eq}–C(5)	H_{ax}–C(6)	2.4	3.0	$H_{pro\text{-}S}$–C(23)	*H*–C(26)	2.8	2.6
H_{eq}–C(5)	H_{ax}–C(6)	2.4		$H_{pro\text{-}R}$–C(23)	Me(37)	3.9	4.6
H_{eq}–C(6)	Me(35)		4.7	$H_{pro\text{-}R}$–C(23)	Me(41)	2.5	3.1
O*H*–C(10)	H_{ax}–C(12)	4.5	4.2	$H_{pro\text{-}S}$–C(23)	Me(41)	2.8	
O*H*–C(10)	*H*–C(14)	3.6	2.7	*H*–C(24)	*H*–C(25)	2.4	
O*H*–C(10)	$H_{pro\text{-}S}$–C(18)		4.2	*H*–C(24)	*H*–C(26)	3.1	3.4
O*H*–C(10)	Me(35)	3.3	3.6	*H*–C(24)	Me(41)	2.9	2.9
O*H*–C(10)	Me(37)	3.1	2.7	*H*–C(25)	*H*–C(26)	2.6	2.5
H–C(11)	*H*–C(13)		2.6	*H*–C(25)	Me(41)		2.5
H–C(11)	Me(35)		2.4	*H*–C(26)	*H*–C(28)	2.6	3.7
H–C(11)	Me(44)		3.0	*H*–C(26)	Me(41)	3.0	3.1
H_{ax}–C(12)	*H*–C(14)	2.4	3.0	*H*–C(26)	Me(42)	2.5	2.5
H_{ax}–C(12)	Me(35)		3.1	*H*–C(28)	H_{ax}–C(30)	2.7	
H_{eq}–C(12)	*H*–C(13)		2.6	*H*–C(28)	H_{eq}–C(30)	3.6	3.4
H_{eq}–C(12)	*H*–C(14)	3.4		*H*–C(28)	H_{ax}–C(34)	2.6	3.0
H_{eq}–C(12)	Me(35)		2.9	*H*–C(28)	Me(41)	3.5	3.1
H–C(14)	*H*–C(17)	2.2	2.3	*H*–C(28)	Me(42)	3.2	3.5
H–C(14)	Me(36)	4.2		*H*–C(28)	Me(45)	4.1	
H–C(14)	Me(37)		2.6	*H*–C(29)	*H*–C(31)	2.3	2.3
H–C(15)	$H_{pro\text{-}R}$–C(16)		2.8	*H*–C(29)	H_{eq}–C(33)	2.4	
H–C(15)	*H*–C(17)	3.5		*H*–C(29)	Me(42)	2.2	2.3
H–C(15)	Me(36)	3.0	2.8	H_{eq}–C(30)	Me(45)	3.0	3.1
H–C(15)	Me(44)	2.6	2.6	Me(41)	Me(42)	2.8	

[a]) The numbering of the heavy atoms is from the *Cambridge Data Bank* coordinate file.

known geometry and distances using the two-spin approximation. These distances were then utilized as restraints within molecular-mechanics calculations for the energetic refinement of the two isomers of FK506 (**2**).

The average and standard deviations of selected dihedrals of the major (*cis*) and minor (*trans*) isomers of **2** from the restrained MD simulations are given in *Table 7*. Comparing the crystal-structure dihedrals (*Table 7*) with that of the major *cis*-isomer reveals significant differences located near the CH_2(23) group (C(20)–C(21),

Table 7. *Averages and Standard Deviations of Selected Dihedrals* τ[°] *of the* trans- *and* cis-*Isomers of FK506* (**2**) *from NOE-Restrained Molecular-Dynamics Simulations*[a])

Torsion	τ of *trans*-Isomer (minor)		τ of *cis*-Isomer (major)		τ from X-ray of **2** (*cis*)[b])
	Average angle	Standard deviation	Average angle	Standard deviation	
C(26)–O(1)–C(1)–C(2)	–168	11	160	9.9	172
O(1)–C(1)–C(2)–C(3)	42	17	–59	19	–80
C(1)–C(2)–C(3)–C(4)	–83	7.1	–84	14	–76
C(2)–C(3)–C(4)–C(5)	–46	13	–50	14	–52
C(3)–C(4)–C(5)–C(6)	41	24	52	13	56
C(4)–C(5)–C(6)–N(7)	–39	27	–50	12	–53
C(5)–C(6)–N(7)–C(2)	42	17	47	9.7	50
C(6)–N(7)–C(2)–C(3)	–45	9.2	–44	9.3	–47
C(2)–N(7)–C(8)–C(9)	180	7.8	–2	7.7	1
N(7)–C(8)–C(9)–C(10)	–95	9.2	–94	7.8	–95
C(8)–C(9)–C(10)–C(11)	176	12	–45	17	–28
C(9)–C(10)–C(11)–C(12)	162	7.3	163	8.6	164
C(10)–C(11)–C(12)–C(13)	–51	7.5	–48	7.6	–54
C(11)–C(12)–C(13)–C(14)	53	7.3	52	7.4	58
C(12)–C(13)–C(14)–C(15)	–172	7.2	–176	7.0	–175
C(13)–C(14)–C(15)–C(16)	–173	7.8	–177	8.9	–178
C(14)–C(15)–C(16)–C(17)	64	8.7	73	10	68
C(15)–C(16)–C(17)–C(18)	–103	15	–162	8.8	172
C(16)–C(17)–C(18)–C(19)	160	8.4	76	14	66
C(17)–C(18)–C(19)–C(20)	108	15	–174	14	–132
C(18)–C(19)–C(20)–C(21)	178	10	176	12	–168
C(19)–C(20)–C(21)–C(22)	–134	15	–76	18	–141
C(20)–C(21)–C(22)–C(23)	100	14	2	34	137
C(20)–C(21)–C(38)–C(39)	70	13	–143	48	174
C(21)–C(22)–C(23)–C(24)	–115	12	–106	30	–118
C(22)–C(23)–C(24)–C(25)	65	9.7	160	20	59
C(23)–C(24)–C(25)–C(26)	–178	11	58	11	–168
C(24)–C(25)–C(26)–C(27)	52	9.4	149	12	56
C(25)–C(26)–C(27)–C(28)	–146	13	91	11	–128
C(26)–C(27)–C(28)–C(29)	–176	11	–174	11	180
C(27)–C(28)–C(29)–C(30)	109	29	115	27	100
C(28)–C(29)–C(30)–C(31)	180	8.2	179	7.5	176
C(29)–C(30)–C(31)–C(32)	–54	6.8	–53	7.0	–56
C(30)–C(31)–C(32)–C(33)	53	6.5	52	7.1	62
C(31)–C(32)–C(33)–C(34)	–53	7.6	–53	7.4	–62
C(32)–C(33)–C(34)–C(29)	53	7.5	53	7.9	59
C(33)–C(34)–C(29)–C(30)	–54	7.1	–52	8.4	–55

[a]) The dihedrals are defined using the numbering of the heavy atoms from the *Cambridge Data Bank*.
[b]) Dihedrals from the crystal structure [5].

C(21)–C(22), C(22)–C(23), C(24)–C(25), and C(26)–C(27)). In the region of the other two CH_2 groups, there are no significant differences. The torsions predicted from the coupling constants are in agreement with the average structure, except for the torsion about C(21)–C(38) where an angle of −143° is found (*Table 7*), while a +60° rotamer was calculated (*Table 5*). However, since this torsion is exocyclic, the standard deviation is quite large, indicating conformational mobility and transitions between rotamers. The average structure from the restrained MD of the major isomer after energy minimization is shown in *Fig. 7a*.

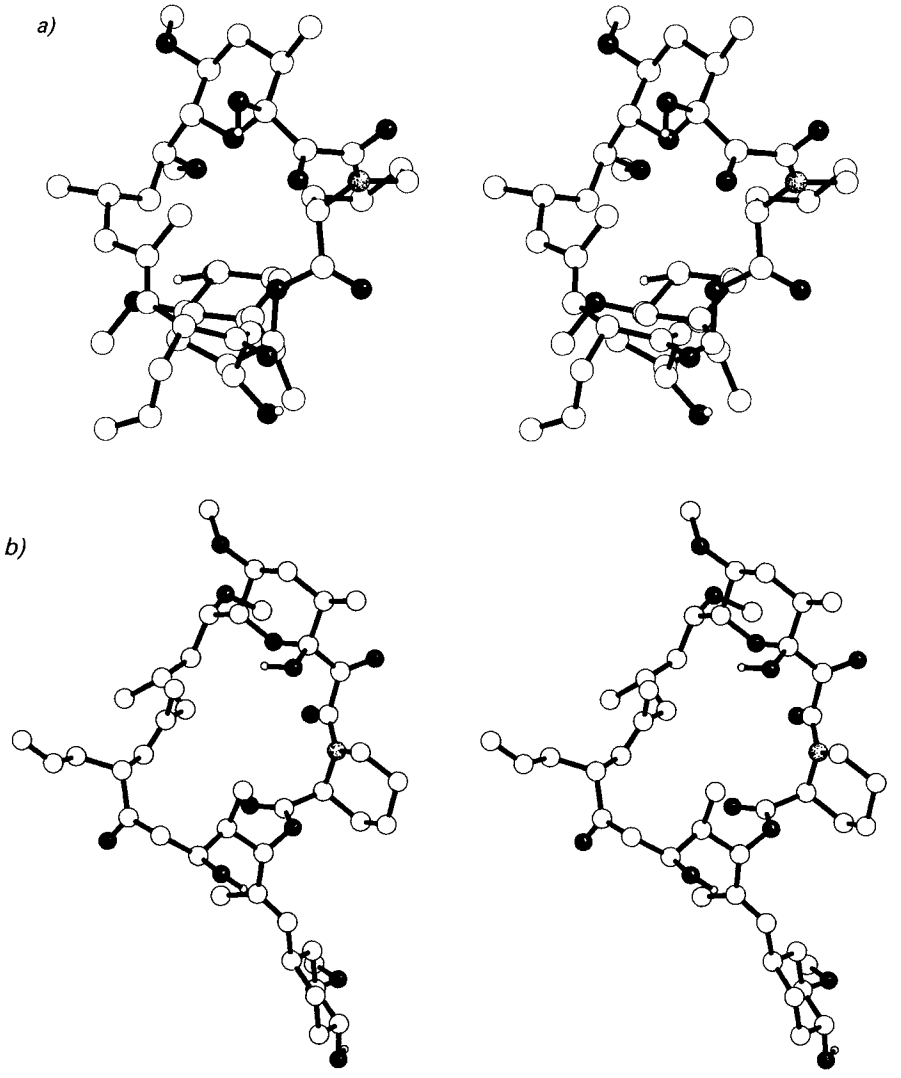

Fig. 7. *Stereoplots of the partially minimized average structure from 100 ps of restrained molecular-dynamics simulations* in vacuo *of the isomers of FK506* (**2**): a) *major isomer, with* cis *amide bond;* b) *minor isomer, with* trans *amide bond*

During the simulation of the minor *trans*-isomer of **2**, conformational changes are localized in the region of the CH_2(16) and CH_2(18) groups, while only small differences are found near the CH_2(23) group. The torsion angle C(8)–C(9)–C(10)–C(11) which started at a value of −28° (the value observed in the X-ray structure of **2**) changes to a *trans*-orientation (average value of 176°). The observed change of this torsion is not caused by the NOE's: a MD simulation with the same starting structure but without application of NOE restraints, resulted in the same transition. The negative *gauche* orientation of this torsion, observed in the crystal structures of FK506 (**2**) and rapamycin (**3**) may arise from packing forces within the solid state. The O(1)–C(1)–C(2)–C(3) torsion angle also changes, from the 119° found in the solid state of **3** (*trans*) to an average value of 42° for the *trans*-isomer of **2**. The torsion angles calculated from the coupling constants of the minor isomer are observed, except for the C(24)–C(25)–C(26)–C(27) torsion which has an average value of 52° (*Table 7*) instead of the predicted value of 180° (*Table 5*). The prediction of a torsion of close to 0° from the large geminal coupling constant is also not found in the MD simulation (average value of −115°). The average structure from the restrained MD of the minor isomer after energy minimization is shown in *Fig. 7b*.

In our previous study [28], the ester torsion (atoms C(26)–O(1)–C(1)–C(2)) of the minor conformation always adopted a *cis*-orientation when the NOE's were applied (NOE-restrained MD). Without the application of the NOE's, the more favored *trans*-orientation [48] was maintained. In the present simulations, the *trans*-orientation is found. However, if the ester is adjusted to the *cis*-orientation, it remains there during NOE-restrained MD, indicating that the NOE's are not sufficient to differentiate between the two orientations about the ester. The difference here and the previous simulation is that all of the NOE's are assigned to specific atoms (*e.g.* the C-atom of Me groups is used) instead of using the wild card facility within DISCOVER which should indicate the average position of all protons of a specific moiety (*e.g.* H*–C(23) for the average position of H–C(23) and H′–C(23)). We now believe that the erroneous use of wild cards to assign the NOE's resulted in the *cis*-ester torsion previously reported.

Conclusions. – The conformations of the major and minor isomers of FK506 (**2**) in $CDCl_3$ have been refined from our previous examination [28] by utilizing the configurational assignments (*pro-R* or *pro-S*) of the methylene protons at C(16), C(18), and C(23) and the application of the NOE's involving these protons. The latest NMR techniques were used to unambiguously assign all ^{1}H- and ^{13}C-NMR shifts and extract many hetero- and homonuclear coupling constants. The refined conformations are necessary for the understanding of the biological action of this family of important drugs.

The data presented here are not only important for refining the structures in solution but will provide valuable assistance in the interpretation of the NMR investigation of complexes of these drugs with their binding proteins currently in progress [49] [59]. The examination of the drug while bound in conjunction with highly refined structures free in solution will provide a clearer picture of the biological actions of the immunosuppressants.

We gratefully acknowledge stimulating discussions with Dr. *David Donald* at *Fisons*, UK. We thank the *Fulbright Commission* for a research award to *D.F.M.*, the *Alexander-von-Humboldt-Stiftung* for a fellowship to *P.K.*, and the *Deutsche Forschungsgemeinschaft* and the *Fonds der Chemischen Industrie* for financial support. The sample of *FK506* was graciously supplied by *Fujisawa Pharmaceuticals* of Osaka, Japan.

REFERENCES

[1] M. Dreyfuss, E. Härri, H. Hofmann, H. Kobel, W. Pache, H. Tscherter, *Eur. J. Appl. Microbiol.* **1976,** *3,* 125.
[2] R. Traber, M. Kuhn, A. Rüegger, H. Lichti, H.-R. Loosli, A. von Wartburg, *Helv. Chim. Acta* **1977,** *60,* 1247.
[3] R. M. Wenger, *Angew. Chem. Int. Ed.* **1985,** *24,* 77.
[4] a) H. Kessler, H. R. Loosli, H. Oschkinat, *Helv. Chim. Acta* **1985,** *68,* 661; b) H. R. Loosli, H. Kessler, H. Oschkinat, H. P. Weber, T. J. Petscher, A. Widmer, *ibid.* **1985,** *68,* 682; c) H. Kessler, M. Köck, T. Wein, M. Gehrke, *ibid.* **1990,** *73,* 1818.
[5] H. Tanaka, A. Kuroda, H. Marusawa, H. Hatanaka, T. Kino, T. Goto, M. Hashimoto, T. Taga, *J. Am. Chem. Soc.* **1987,** *109,* 5031.
[6] T. Kino, H. Hatanaka, M. Hashimoto, T. Goto, M. Okuhara, M. Kohsaka, H. Aoki, H. Imanaka, *J. Antibiot.* **1987,** *40,* 1249.
[7] T. Taga, H. Tanaka, T. Godo, S. Tada, *Acta Crystallogr., Sect. C* **1987,** *43,* 751.
[8] F. L. Dumont, M. J. Staruch, S. L. Koprak, M. R. Melino, N. H. Sigal, *J. Immunol.* **1990,** *144,* 251.
[9] E. A. Emmel, C. L. Verweij, D. B. Durand, K. M. Higgins, E. Lacy, G. R. Crabtree, *Science* **1989,** *246,* 1617.
[10] S. N. Sehgal, H. Baker, C. Vezina, *J. Antibiot.* **1975,** *27,* 727.
[11] D. C. N. Swindells, P. S. White, J. A. Findlay, *Can. J. Chem.* **1977,** *56,* 2491.
[12] J. A. Findlay, L. Radics, *Can. J. Chem.* **1980,** *58,* 579.
[13] G. Fischer, H. Bang, C. Mech, *Biomed. Biochem. Acta* **1984,** *43,* 1101.
[14] R. F. Standaert, A. Galat, G. L. Verdine, S. L. Schreiber, *Nature (London)* **1990,** *346,* 671.
[15] M. Tropschug, E. Wachter, S. Mayer, E. R. Schönbrunner, F. X. Schmid, *Nature (London)* **1990,** *346,* 674.
[16] R. E. Handschumacher, M. W. Harding, J. Rice, R. J. Drugge, S. L. Speicher, *Science* **1984,** *226,* 544.
[17] M. W. Harding, R. E. Handschumacher, S. L. Speicher, *J. Biol. Chem.* **1986,** *261,* 8547.
[18] R. B. Freedman, *Nature (London)* **989,** *341,* 692.
[19] M. W. Harding, A. Galat, D. E. Uehling, S. L. Schreiber, *Nature (London)* **1989,** *341,* 758.
[20] J. J. Siekierka, S. H. Y. Hung, M. Poe, C. S. Lin, N. H. Sigal, *Nature (London)* **1989,** *341,* 755.
[21] N. Takahasi, T. Hayano, M. Suzuki, *Nature (London)* **1989,** *337,* 473.
[22] G. Fischer, B. Wittmann-Liebold, K. Lang, T. Kiefhaber, F. X. Schmid, *Nature (London)* **1989,** *337,* 476.
[23] R. K. Harrison, R. L. Stein, *Biochemistry* **1990,** *29,* 3813.
[24] R. K. Harrison, R. L. Stein, *Biochemistry* **1990,** *29,* 1684.
[25] B. E. Bierer, P. K. Somers, T. J. Wandless, S. J. Burakoff, S. L. Schreiber, *Science* **1990,** *250,* 556.
[26] S. L. Schreiber, *Science* **1991,** *251,* 283.
[27] H. Fretz, M. A. Albers, A. Galat, R. F. Standaert, W. S. Lane, S. J. Burakoff, B. E. Bierer, S. L. Schreiber, *J. Am. Chem.* **1991,** *113,* 1409.
[28] P. Karuso, H. Kessler, D. F. Mierke, *J. Am. Chem. Soc.* **1990,** *112,* 9434.
[29] H. Kessler, R. Hässner, W. Schüler, in preparation.
[30] a) L. Braunschweiler, R. R. Ernst, *J. Magn. Reson.* **1983,** *53,* 521; b) D. G. Davis, A. Bax, *Am. Chem. Soc.* **1985,** *107,* 2820.
[31] A. Bax, D. G. Davis, *J. Magn. Reson.* **1985,** *65,* 355.
[32] a) A. A. Bothner-By, R. L. Stephens, J. Lee, C. D. Warren, R. W. Jeanloz, *J. Am. Chem. Soc.* **1984,** *106,* 811; b) A. Bax, D. G. Davis, *J. Magn. Reson.* **1985,** *63,* 207; c) H. Kessler, G. Griesinger, R. Kerssebaum, K. Wagner, R. R. Ernst, *J. Am. Chem. Soc.* **1987,** *109,* 607.
[33] a) J. Jeener, B. H. Meier, P. Bachmann, R. R. Ernst, *J. Chem. Phys.* **1979,** *71,* 4546; b) S. Macura, Y. Huang, D. Suter, R. R. Ernst, *J. Magn. Reson.* **1981,** *43,* 259.
[34] a) C. Griesinger, O. W. Sørensen, R. R. Ernst, *J. Am. Chem. Soc.* **1985,** *107,* 6394; b) C. Griesinger, O. W. Sørensen, R. R. Ernst, *J. Chem. Phys.* **1986,** *85,* 6837; c) C. Griesinger, O. W. Sørensen, R. R. Ernst, *J. Magn. Reson.* **1987,** *75,* 474.
[35] a) L. Müller, *J. Am. Chem. Soc.* **1979,** *101,* 4481; b) A. Bax, R. H. Griffey, L. B. Hawkins, *J. Magn. Reson.* **1983,** *55,* 301; c) A. Bax, S. Subramanian, *ibid.* **1986,** *67,* 565.
[36] H. Kessler, P. Schmieder, M. Kurz, *J. Magn. Reson.* **1989,** *85,* 400.

[37] G. Bodenhausen, D. L. Ruben, *Chem. Phys. Lett.* **1980,** *69,* 185.
[38] H. Kessler, P. Schmieder, H. Oschkinat, *J. Am. Chem. Soc.* **1990,** *112,* 8599.
[39] P. Schmieder, M. Kurz, H. Kessler, submitted to *J. Biomol. NMR.*
[40] A. T. Hagler, in 'The Peptides', Eds. S. Udenfriend, J. Meienhofer, and V. Hruby, Academic Press, Orlando, FL, Vol. 7, 1985, pp. 214–296.
[41] a) S. L. Weiner, P. A. Kollman, D. A. Case, U. Chandra Singh, C. Ghio, G. Alagona, S. Profeta, P. Weiner, *J. Am. Chem. Soc.* **1984,** *106,* 765; b) F. A. Momany, R. F. McGuire, A. W. Burgess, H. A. Scheraga, *J. Phys. Chem.* **1975,** *79,* 2361; c) W. F. van Gunsteren, H. J. C. Berendsen, 'Groningen Molecular Simulation (GROMOS) Library Manual', Biomos B. V., Nijenborgh 16, NL 9747 AG Groningen, pp. 1–229.
[42] T. M. G. Koning, R. Boelens, R. Kaptein, *J. Magn. Reson.* **1990,** *90,* 111.
[43] R. Fletcher, 'Practical Methods of Optimization', John Wiley, New York, 1980, Vol 1.
[44] A. S. Edison, W. M. Westler, J. L. Markley, *J. Magn. Reson.* **1991,** *92,* 434.
[45] P. Schmieder, H. Kessler, H. Oschkinat, *Angew. Chem. Int. Ed.* **1990,** *29,* 546.
[46] J. J. Titman, J. Keeler, *J. Magn. Reson.* **1990,** *89,* 640.
[47] G. T. Montelione, M. E. Winkler, P. Rauenbuehler, G. Wagner, *J. Magn. Reson.* **1989,** *82,* 198.
[48] G. Quinkert, N. Heim, J. Glenneberg, U. Döller, M. Eichhorn, U.-T. Billhardt, C. Schwarz, G. Zimmermann, J. W. Bats, G. Dürner, *Helv. Chim. Acta* **1988,** *71,* 1719.
[49] S. W. Fesik, R. T. Gampe, T. F. Holzman, D. A. Egan, R. Edalji, J. R. Luly, R. Simmer, R. Helfrich, V. Kishore, D. H. Rich, *Science* **1990,** *250,* 1406.
[50] T. J. Wandless, S. W. Michnick, M. K. Rosen, M. Karplus, S. L. Schreiber, *J. Am. Chem. Soc.* **1991,** *113,* 2339.